Jordan S, Baker NJ.

Design and Build of a Mass Critical, Air-cooled Transverse Flux Machine for Aerospace.

In: 2016 XXII International Conference on Electrical Machines (ICEM). 2016, Lausanne, Switzerland: IEEE

DOI link to article:

http://dx.doi.org/10.1109/ICELMACH.2016.7732715

Date deposited:

07/12/2016

Design of an Air-cooled Transverse Flux Machine for Aerospace Applications

Steven Jordan, Nick J. Baker

[Φ]***Abstract* -- Electric motors are becoming increasingly utilized in aircraft, replacing traditionally mechanical or hydraulic auxiliary systems to realize improvements in mass, control and efficiency. Aerospace motor design has the unique characteristic that mass and, therefore, torque density is of critical importance. For low maintenance, non-safety critical components, which are only used for short durations of the flight cycle, efficiency also becomes less important, whilst eliminating an external cooling circuit and gearbox will benefit mass constraints. In order to meet a stringent mass target, this paper considers the design of a high torque density machine suitable for a low speed aerospace application. As mass is reduced, thermal capability becomes critical and thermal simulations are presented for operational characteristics.**

***Index Terms* -- Transverse Flux Machine, Torque Dense, Aerospace Applications**

I. Introduction

The aerospace sector has seen significant developments in recent years. European climate change targets [1] have led to modifications in aircraft architecture in order to achieve greater fuel efficiency: mass reduction can have a significant impact on this and, as a result, lightweight composites are now widely used in the construction of aircraft [2, 3]. Furthermore, electrical systems are being utilized in replacing the auxiliary loads traditionally supplied by hydraulic or mechanical systems. For all aspects of airframe design there exist strict constraints on mass, where excess yields an increase in fuel burn. If a motor drive system is only to be used for seconds to minutes then this can have a significant impact on overall efficiency. It is critical, therefore, in the design of motors that mass is kept to a minimum without impeding performance.

Transverse flux machines (TFM) are well known for their torque dense properties: where the stator teeth act to create a number of poles which have an MMF equal to that of the circumferential coil they encompass. The structure allows for a high pole number yielding high air-gap field strengths and, coupled with a greater magnetic loading in the rotor, this results in a greater specific torque output when compared with typical radial and axial flux variants [4, 5]. However, three-dimensional flux paths prove problematic in their design and increase the complexity in manufacturing. Furthermore, power converters must be rated in accordance with the motor's high reactance.

Motor heating can be a critical issue and thermal work is often overlooked in machine design as it is deemed of secondary importance to electromagnetic performance. However, where mass is minimized due to the unique requirements of aerospace applications, thermal considerations become important in ensuring that the machine components are capable of withstanding the internal temperatures generated under operation. Where cooling methods are limited - coolant or oil not being suitable on account of both mass and safety concerns, for example - the need for adequate air flow across heat paths may prove inherently beneficial for a structure such as the TFM where the stator teeth act as cooling vanes around the coil that is relatively exposed to passing air.

This paper relates to an aerospace application where torque density, is of prime importance. The Physical space envelope is limited and there is a necessity to deliver a low mass solution. Rated torque conditions must be delivered for approximately 30 minutes, with an overload torque requirement for 30 seconds. Voltage, current, diameter and axial length are all limited by existing airframe architecture, and there is a desire for a direct-drive, air-cooled solution.

II. Design Study

For this application, high rated torque requirements must be met, with a desire for achieving an overload condition. Existing power converter limitations place added restrictions on the machine, whilst the application also has its inherent constraints with respect to volume and mass, detailed in *Table 1.*

Table 1: Machine Specification

Constraint	Value	Unit
Voltage	< 215	V_{RMS}
Speed	< 450	rpm
Rated Torque	1	p.u.
Overload Torque	3.2	p.u.
Volume	0.025	m^3
Mass	1	p.u.

There exist a number of factors that can change the performance of a TFM. It is common, for simplicity of manufacture, to utilize three single-phase TFMs - offset by 120° electrical - to create what is termed a separate phase machine. Reducing or removing this separation can lead to improvements in torque density but the resultant increase in

[Φ]The project has been jointly financed by SAFRAN and UK Technology Strategy Board funding body Innovate UK.

S. Jordan is with the Electrical Power Group, Newcastle University, Newcastle, NE1 7RU, United Kingdom (e-mail: steven.jordan@ncl.ac.uk).

N. J. Baker is with the Electrical Power Group, Newcastle University, Newcastle, NE1 7RU, United Kingdom (e-mail: nick.baker@mcl.ac.uk).

inductance has a negative impact on the converter rating. Since torque density is a key attribute of this machine, a combined-phase machine is utilized [6, 7].

Typical manufacturing methods would employ soft magnetic composite (SMC) materials, which provide excellent loss reduction capabilities through reduced eddy current paths and low hysteresis at mid- to high-frequency operation. However, their manufactured properties result in a reduced permeability and lower saturation characteristic, when compared with high grade steels, making their use for flux collection in stator poles unfitting. One suitable option is the provision of laminated stator teeth interlocking an SMC core-back [8], depicted in *Figure 1*. This would provide a highly permeable tooth structure with a high saturation point, whilst allowing for three-dimensional flux linking between inter-phase poles. Care must be taken in tolerance requirements with this approach in order to avoid parasitic air-gaps, which can lead to stray losses and localized thermal degradation.

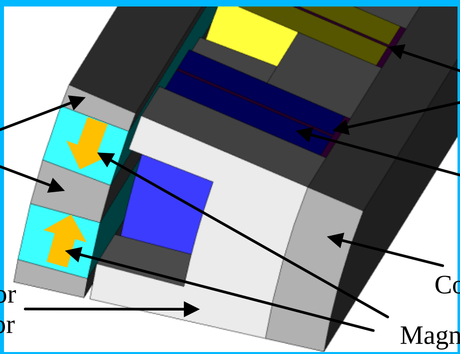

Figure 1: External Rotor TFM Topology

External rotor machines suit high torque applications [9] as the radial length can be utilized to maximize the magnet content and stator outer diameter. For TFMs, this allows a greater pole number without constricting the respective rotor and stator pole arcs. Surface mounted magnets are unsuitable for a low mass machine since a magnetic return path must exist in the form of a core-back, which can be used to form a containment layer. A concentrated flux rotor comprising circumferentially magnetized magnets sandwiched between SMC pole pieces offers the potential to maximize the magnetic loading whilst minimizing rotor mass through a reduction in radial length. Moreover, utilizing a flux concentrating rotor will provide a higher air-gap flux density. However, problems arise with the concentration of the flux saturating the pole pieces and creating leakage paths if the air-gap is too great. Furthermore, the localized magnetic field leads to high cogging and ripple effects which must be mitigated through careful stator design consideration.

The TFM can be designed free of the constraints that impinge radial and axial flux machines. Typically a high pole number is desirable to achieve the torque density through greater magnetic loading, as can be seen in *Table 2*. This is beneficial in low speed applications, where the operating frequency is relatively low. A scripted optimization process was carried out around this key torque producing component within the fixed volume constraints of the specification. The improvement of torque density can be realized by a high pole count but with decreasing benefits at higher numbers.

Table 2: Pole Number Attributes

Pole Pairs	Cogging Torque (%)	Torque Density (Nm/kg)	Ripple Torque (%)
28	11.68	25.06	29.67
32	12.18	27.05	28.07
36	12.10	28.05	29.76
40			
44	12.02	29.60	28.13
48	12.42	30.08	27.73

For a similar sized machine, the ideal stator tooth width to rotor pole width (RPW) is approximately a ratio of 2.1:1 [10]. However, with fixed rotor conditions, simulating across a range of stator tooth widths (STW), based on electrical angle, the optimal ratio was found to be approximately 1.9:1, highlighted in *Table 3*. Furthermore, at a reduced ratio, there was an observed reduction in ripple and savings made with respect to stator mass.

Table 3: Changing Tooth Width with Respect to Rotor Pole Width

Electrical Angle (°)	Ratio (STW:RPW)	Torque (p.u.)	Ripple (%)
120	1.6:1	1.12	44.27
135	1.9:1	1.15	41.46
153	2.1:1	1.12	42.11
160	2.2:1	1.11	40.78
180	2.4:1	1.07	42.58

With a concentrated flux rotor topology, the strong magnetic fields yield a high ripple torque. This is problematic for machines where high shear forces can be exerted on components. Reducing this ripple torque can be achieved through tooth pitching [11], where the stator teeth are separated by an angle greater than the stator arc between the pole pair, depicted in *Figure 2*.

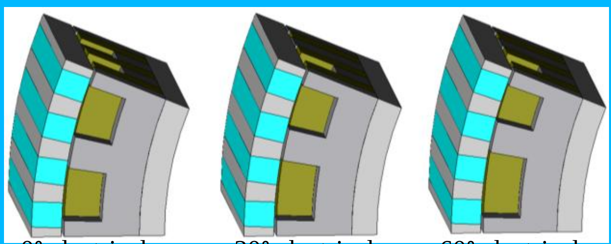

Figure 2: Stator Tooth Pitching

With the teeth pitched, a significant reduction in ripple torque can be achieved, as depicted in *Figure 3*. However, as the pitching angle is increased, the fundamental torque producing component reduces and the average torque value falls below the rated torque requirement. With the modifications previously discussed, a 30° electrical pitching can be sustained whilst still meeting rated conditions and providing some overload capability.

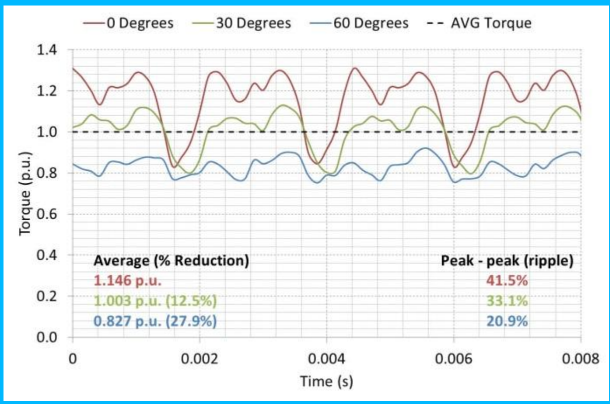

Figure 3: Torque Profiles for Pitched Stator Teeth

From this study, further changes could be made to the geometry to find the optimal configuration. The rotor pole arc is constrained by the magnet material. Fixing the stator geometry whilst varying the magnet content, as a percentage of the rotor pole arc, the optimal was found to be 60% magnet content. The initial proposed magnet material was a high grade NdFeB material, which offered the highest co-energy and residual flux density at working values. However, at higher temperatures this material didn't perform well, further discussed in Section III. The remaining rotor sections are constructed from SMC material, to allow for the flux to permeate in three dimensions. Simulating around the pole arc study found that adding a chamfer angle to the magnets, further increasing their size with respect to the pole piece, provided a marginal gain in air-gap flux density and, therefore, torque output with no increase in mass but a marginally higher ripple rate: observed in *Figure 4*.

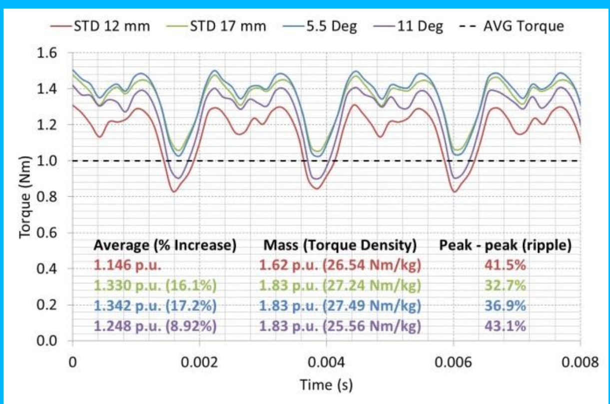

Figure 4: Torque Output for Angled Rotor Magnets

Observing the flux density plots, it is clear that mass savings can be made. Areas of low flux are observed, depicted in *Figure 5*, over an electrical cycle between consecutive teeth.

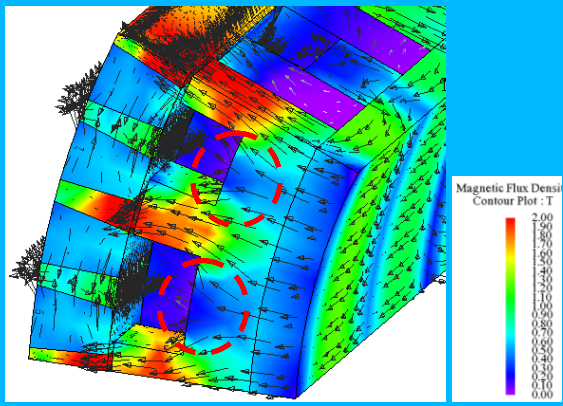

Figure 5: Magnetic Flux Density Plot of TFM Section

This can be removed without compromising the magnetic or structural integrity of the machine: an overall saving of 5 % can be made on active mass.

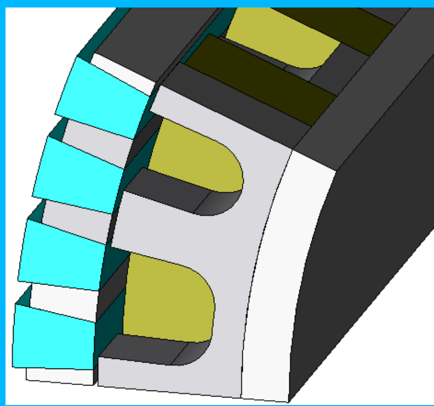
Figure 6: Stator and Rotor with Mass Savings

III. Magnet Material

The relatively low duty cycle that this motor will endure means that a higher current density can be utilized to produce the high electrical field strength, and thus high torque output. However, localized temperatures can exceed operating conditions for some components if not properly considered whilst the high electric fields can act to demagnetize at these temperatures. Prior to the thermal work carried out, a quick study was performed on magnet grades to withstand high temperatures.

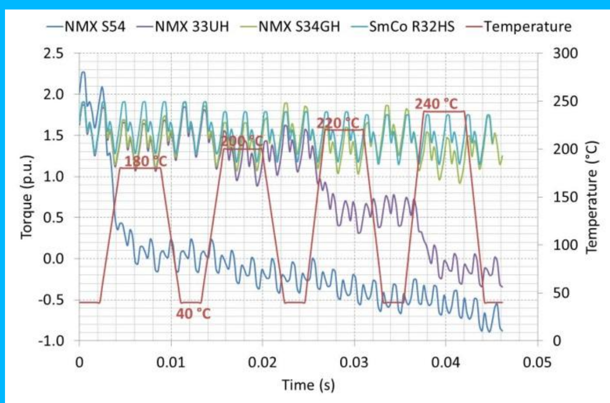

Figure 7: Demagnetization Characteristics at Thermal and Electrical Limits

Initially, a high grade NdFeB magnet type was chosen with a maximum energy product of 54 MGOe and high remnant flux density. However, as *Figure 7* shows, whilst a high torque output is achievable at low temperature operation and with full converter current applied to the windings, the magnet suffers irreversible demagnetization at 180 °C. As the heat handling capability increases, the maximum energy product of the magnet decreases leading to a reduction in torque output. To that end, SmCo magnets may be a more suitable prospect since they outperform high temperature NdFeB grades across a range of operating temperatures.

IV. Winding Material

Winding a TFM is a relatively straightforward process since they are circumferentially wound and tend to have large bend radii. Two winding types were considered across three designs, as shown in *Figure 8*. The first is a typical, small gauge wire (AWG 10) to achieve a high fill factor and, therefore, good thermal behavior. With a cross-sectional area of 5.27 mm^2, the maximum RMS current is limited to approximately 50 A. With adequate cooling though, this can be exceeded for short duty cycle applications.

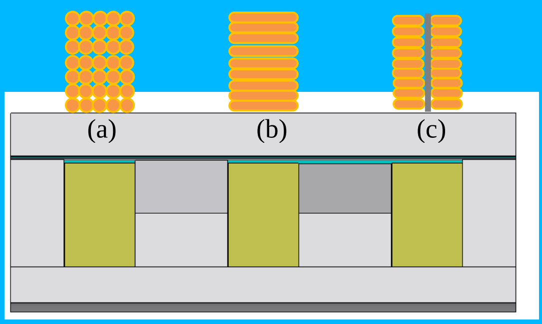

Figure 8: Winding Configurations for TFM

The windings in *Figure 8* (b) and (c) are strip windings which are commonly used in TFMs [12] and still achieve adequate fill factors. However, problems arise with mechanical termination - particularly for (b) - where the bend radius is large, posing significant issues in bringing connections out. For this reason, and the possibility to insert a thermal guide path in the center of the paralleled coils, winding option (c) is chosen.

Further mass savings can be made to both machines through utilizing aluminium windings. The mechanical properties of aluminium make it highly desirable in mass critical applications and the mass density of less than 1/3rd that of copper is a key prospect. However, the penalty is a higher resistivity, which, at 2.7 x 10^{-8} Ω.m, will provide a greater Joule loss when compared with copper. Furthermore, when considering aluminium as a potential winding material and also making savings in active mass, there will be a reduced potential thermal capacity. This can have significant bearings on the performance of the machine under load conditions and at higher duty cycles. The ability for the machine to absorb heat from losses created is greatly diminished and heat cannot be dissipated through the structure quickly enough to radiate out from the cooling faces. Thermal paths are difficult to define as parasitic air-gaps between components can have a localized insulating effect especially with a modular laminate-SMC construction discussed with the TFM.

Table 4: Peak Temperature Values

	Copper	Aluminium
TFM	205	353
Air-cored	350	440

V. Thermal Modelling

The electromagnetic solution results gathered from JMAG are used in the thermal finite element analysis study in the same software environment. The losses are computed as winding Joule losses, with time dependent eddy current and hysteresis losses. These can be time-averaged and used in calculating the temperature rise in the meshed elements. Boundary conditions are placed between surfaces, providing a thermal transfer coefficient surface area to air: a casing is also specified with transfer boundary conditions and a thermal resistance between the air and casing, where the ambient air is at a reference temperature of 40 °C. Frictional losses such as windage and bearing vibration are assumed to be zero.

The Joule loss in the conducting coils can be found from the I^{2}R losses, the dominant effect in generation of heat losses. Skin effect is neglected since the electrical frequency and higher harmonic content are not excessive. The coils will have a thermal resistance associated with the insulation to encapsulate the windings. The winding is assumed to have an insulation layer of 0.1 mm and the thermal conductivity of the insulation (Kapton®) is 0.46 W/m/°C.

For an air-gap of 1 mm, the heat transfer coefficient of the stator and rotor surfaces to the air-gap will be different to a static boundary condition. It can be calculated using the following formula [13]:

$$h = \frac{6.6}{10^5} \frac{vr^{0.67}}{l_g{}^{0.33}} \times 10^4 \quad (1)$$

where h is the heat transfer coefficient in W/m^2/°C, vr is the velocity radius in cm/s and l_g is the air-gap in cm, a multiplier is used to correct for units chosen.

Other transfer boundaries are interfacing with air and thus have a constant heat transfer coefficient of between 5 and 25 W/m^2/°C through natural convection. Since there is air-flowing across and through the machine it is assumed that the transfer to air will be at the upper boundary.

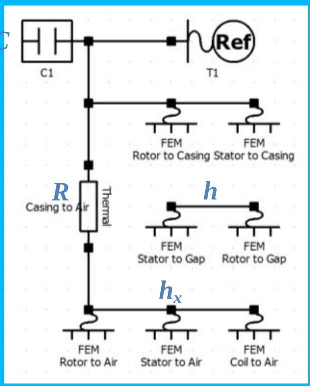

Figure 9: Thermal Circuit for TFM

The casing can be modelled as a thermal capacitance based on its volumetric envelope and material properties. For this application it is important to ensure the thermal performance of the stator since the coils are expected to produce the greatest amount of heat. The casing interfaces the stator internal bore and the faces of the outer stator teeth. An allowance of 5 mm thickness has been accounted for in the specification.

Assuming the material is steel with a specific heat capacity C_p of 465 J/kg/°C and a density ρ of 7760 kg/m^3, the capacitance C of the casing can be calculated:

$$C = \frac{V}{32} C_p \rho \tag{2}$$

There exists a thermal resistance R between the air and the casing of the machine. The surface area A (mm^2) and the heat transfer from the surface h_x (W/m^2/°C) can be used to calculate this resistance:

$$R = \frac{1}{A \cdot h_x} \times 10^6 \tag{3}$$

The resultant thermal boundary conditions for the thermal modelling of the TFM are contained in *Table 5*.

Table 5: Thermal Boundary Values for TFM

	Symbol	Value	Units
Air-gap Heat Transfer Coefficient	h	120	W/m^2/°C
Casing Thermal Capacitance	C	700	J/°C
Casing Thermal Resistance	R	10.87	°C/W
Ambient Heat Transfer Coefficient	h_x	25	W/m^2/°C

The resultant temperature distribution for operation over a 30 minute time period is depicted in *Figure 10*. It indicates that the machine is approaching a thermal limit for winding temperature but that the magnets are within a working temperature for some grades of NdFeB. It is common for isotropic models to underestimate the thermal hot-spot that can occur in the center of the winding, and thus limit the lifetime of the winding: thermocouples will be strategically placed throughout the coils and the machine to monitor temperature variations during operation.

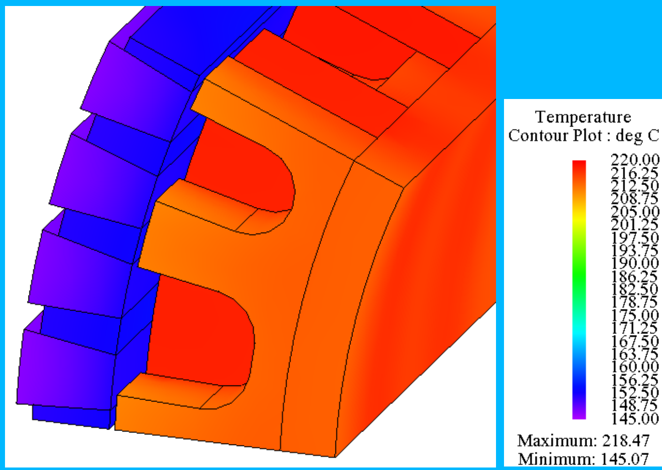

Figure 10: Temperature Distribution through TFM after 30 Minutes

VI. PROTOTYPING


Figure 11: CAD Model of Transverse Flux Machine

The designed TFM, illustrated in *Figure 11*, is currently under construction for testing and comparison with the specification. The electromagnetic simulations indicate that rated torque can be readily achieved but with a limited overload capability due to the stringent mass constraints. The proposed construction combines SMC with laminate cobalt iron to produce a three-phase combined-phase machine.

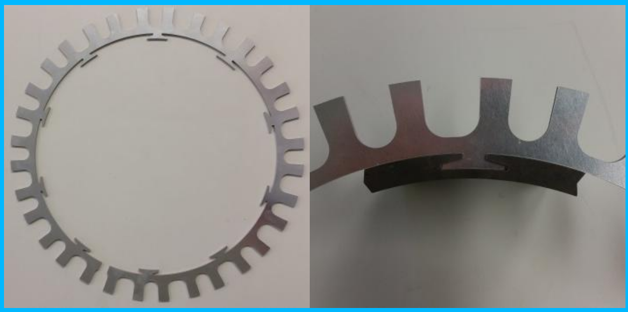

Figure 12: Prototype Laminate Stator Tooth Ring with SMC Core-back

The stator laminated tooth ring, shown in *Figure 12*, is wire-eroded from stock material to check tolerances and accuracy in producing a full phase set for the prototype machine. Parasitic air-gaps between interfacing components, such as, in this case, the SMC core-back and stator laminations, must be minimized to reduce their impact on the electromagnetic and thermal performance of the motor. A circumferential gap is incorporated in the stator laminations to remove the eddy current path whilst also allowing for the coil windings to exit via the SMC core-back.

Table 6: Prototype Machine Construction

Component	Material	Grade
Core-back	SMC	5P 700
Laminated teeth	Cobalt iron	Vacoflux® 50 (or equivalent)
Pole pieces	SMC	5P 700
Magnets	Samarium Cobalt/ NdFeB	Recoma R32 or greater/N35 EH/UH
Winding	Copper strip	IACS 92% with Kapton® insulation

The proposed materials contained in *Table 6* are ideal and based on the simulation results. Obtaining SMC grades of 5P for the core-back and pole pieces would require the design and fabrication of separate pressing tools. This is not suitable for a prototype machine and, therefore, a prototyping material, which can be machined, is more suitable at this stage. This will impact on the performance of the motor since the permeability and saturation characteristics change. Moreover, cobalt iron laminations may be inhibitive in terms of material expenditure and, as a result, a different material may be required. Silicon iron is a much more cost effective replacement but with a poorer saturation point when compared with cobalt iron, providing a torque density of 26.13 Nm/kg. Any compromises made in the prototype machine can be validated and provide a platform for the mass manufacture of the original design.

VII. Conclusions

This paper proposes a high torque density, low speed machine for use in an aerospace application. Since mass is a critical target, it is minimized with respect to meeting the rated torque requirements through a design study to achieve maximum torque. However, overload torque is limited as a result of the reduction in active material, leading to earlier saturation. Furthermore, it was shown that whilst the thermal handling capability is decreased with mass reduction, the performance of the machine remains within tolerable limits for the component parts. Torque ripple is reduced via stator tooth pitching, reducing the ripple by approximately 9 %. A prototype is currently under construction to validate the electromagnetic and thermal modelling.

The final full paper will contain more detail regarding the procurement, manufacturing and any subsequent geometry changes in component parts.

VIII. Acknowledgment

The authors would like to acknowledge the support of SAFRAN and Innovate UK partners MTD Ltd., MEP, Teesside University and Arnold Magnetics. Furthermore, thanks goes to JSOL for supplying finite element modelling program JMAG.

IX. References

[1] European Environment Agency, European Aviation Safety Agency, and Eurocontrol, "European Aviation Environmental Report" in 2016.

[2] Airbus, "Environmental Innovations" in *Sustainable Aviation*, France, 2013.

[3] Boeing, "Environment Report 2014," Available at: http://www.boeing.com/aboutus/environment/environment_report_14/ [Accessed: 12th February 2016]

[4] J. F. Gieras, *Permanent Magnet Motor Technology*, Third ed.: CRC Press, 2009.

[5] S. Jordan and N. J. Baker, "Air-Cooled, High Torque Machines for Aerospace Applications," in *8h IET Conference on Power Electronics, Machines and Drives*, Glasgow, Scotland, UK, 2016.

[6] J. G. Washington, G. J. Atkinson, N. J. Baker, A. G. Jack, B. C. Mecrow, B. B. Jensen, *et al.*, "Three-Phase Modulated Pole Machine Topologies Utilizing Mutual Flux Paths," *IEEE Transactions on Energy Conversion*, vol. 27, pp. 507-515, 2012.

[7] J. G. Washington, G. J. Atkinson, N. J. Baker, A. G. Jack, B. C. Mecrow, B. B. Jensen, *et al.*, "An Improved Torque Density Modulated Pole Machine for Low Speed High Torque Applications," in *6th IET International Conference on Power Electronics, Machines and Drives*, 2012, pp. 1-6.

[8] H. M. Amreiz, "Difficulties and Complexities Encountered in the Design of Transverse Flux Machines," in *Electrical Systems for Aircraft, Railway and Ship Propulsion*, 2012, pp. 1-6.

[9] T. Reichert, T. Nussbaumer, and J. W. Kolar, "Torque Scaling Laws for Interior and Exterior Rotor Permanent Magnet Machines," in *Intermag Proceedings*, Sacramento, CA, 2009.

[10] L. Ji-Young, C. Jung-Hwan, K. Do-Hyun, K. Sung-Il, and H. Jung-Pyo, "Tooth Shape Optimization for Cogging Torque Reduction of Transverse Flux Rotary Motor Using Design of Experiment and Response Surface Methodology," *IEEE Transactions on Magnetics*, vol. 43, pp. 1817-1820, 2007.

[11] J. G. Washington, G. J. Atkinson, and N. J. Baker, "Reduction of Cogging Torque and EMF Harmonics in Modulated Pole Machines," *IEEE Transactions on Energy Conversion*, vol. PP, pp. 1-10, 2016.

[12] B. C. Mecrow, A. G. Jack, and C. P. Maddison, "Permanent Magnet Machines for High Torque, Low Speed Applications," in *International Conference on Electrical Machines*, 1996, pp. 461-466.

[13] D. Farnia and T. Hattori, "Electro-machanical Simulation of a Permanent Magnet Brushless DC Motor," in *JMAG Users Conference*, 2006.

X. BIOGRAPHIES

Steven Jordan received the M.Eng. and Ph.D. degrees from the University of Manchester, Manchester, U.K., in 2009 and 2013, respectively. He qualified as an apprentice engineer with Jaguar Cars Ltd. before undertaking his further studies. He was elected Whitworth Scholar and Whitworth Senior Scholar on completion of his respective degrees. He is currently a Research Associate with Newcastle University, Newcastle upon Tyne, U.K., where his main research interests include the design, simulation, and finite element modeling of machines and drives for aerospace and vehicle applications.

Nick J. Baker received the M.Eng. degree in mechanical engineering from Birmingham University, Birmingham, U.K., in 1999, and the Ph.D. in electrical machine design for marine renewable energy devices from Durham University, Durham, U.K., in 2003. He was a Researcher of Machine Design at Durham University in addition to academic posts within Lancaster University's Renewable Energy Group (2005–2008), and currently Newcastle University's Electrical Power Group. He has spent a period in industry as a Senior Consultant for energy consultancy TNEI Services, Ltd., Newcastle, U.K., from 2008 to 2010. He is currently working on machines across the renewable, automotive, and aerospace sectors.